Civil Engineering Infrastructures Journal xx,xx
DOI: 10.22059/ceij.2025.383449.2168

Experimental Investigation of Short Concrete-Filled Lightly Reinforced RPC Compression Members under Edge Load

#	Name	Email Address	Position	Country	Affiliation
1	Ali, Ammar	ammar.a.ali@uotechnology.edu.iq	Professor	Iraq	Civil Engineering Department, University of Technology, Baghdad, Iraq
2	mahdi, fadhil	mahdifadhil049@gmail.com	Other	Iraq	Department of Civil Engineering, University of Technology, Baghdad, Iraq

Received: 27/12/2024

Revised: 12/02/2025

Accepted: 18/03/2025

ABSTRACT: This study investigates the effect of the unsymmetrical loading on compression members like columns and piers of bridges. The edge loads are subjected directly on only one side of the cross-section of the compression member. The behavior of solid columns and hollow reactive powder concrete RPC columns with normal concrete NC filling was investigated. To explore the role of the reinforcement on this novel type of compression members both reinforced and unreinforced specimens were tested. The hollow precast RPC shells were of various thicknesses along with the solid columns. The deflection and strain responses were plotted and failure modes were recorded. It was found that increasing the thicknesses of the RPC walls from 25 mm to 50 mm led to an increase in the ultimate load by approximately 10%. A brittle failure was observed in all specimens, and the crack loads were close to the ultimate loads. Increasing the lateral reinforcement ratio of the specimens enhances the strength effectively. The significance of the present study is to investigate the behavior of the hybrid members manufactured from different grades of concrete under the action of the edge loads as in the case of bridge piers and precast construction.

Keywords: short members, hybrid column, edge load, RPC, NC

1. Introduction

The reactive powder concrete RPC is an ultrahigh strength concrete with very fine constituent materials and is classified as an ultrahigh performance concrete UHPC. RPC contains a high quantity of steel fibers leading to high ductility and energy dissipation characteristics (Wang et al., 2021). RPC mix includes a high percentage of cement, a low water/binder ratio, a high superplasticizer dosage, an extra fine crushed quartz, and silica fume (Salahuddin et al., 2020). This type of concrete includes high-performance properties, such as limited shrinkage, low permeability, and high durability (Moslehi, et al., 2023). The ultra-high strength type of concrete like RPC allows increasing the maximum steel reinforcement ratios set by the standards. On the other hand, the presence of high percentages of steel fiber content and raising the tensile strength encourages lowering the steel reinforcement ratios or even using non-reinforced members. The forming of structural elements with the lowest ratios of reinforcement in columns or beams can be seen in the footbridge of Sherbrooke, Canada, where the chords of the truss were unreinforced RPC beams (Blais and Couture, 1999), and also in the Mars Hill bridge, USA, where it composed of I-girders with no shear reinforcement (Abdal, et al., 2023).

On the other hand, the normal concrete NC is a heterogeneous material of constituents ranging from fine cement to coarse aggregates each having different strengths and moduli of elasticity. This means NC will be weak under tensile stresses and can split or disintegrate easily due to internal pressures like freezing and thawing conditions. Eventually, NC will have lower durability and require more reinforcement ratios to resist cracking stresses.

The main disadvantage of RPC is its high cost. This will prompt using of hollow, hybrid, or composite concrete structural elements. Because of the superior properties of RPC, like high durability and strength, the outer shells of the columns preferably can be made up of RPC, while the inner core can be filled with NC. The above allows us to consider the precast hollow RPC tubes as molds to be filled with NC in situ. The bond strength between the different types of concrete can be considered in enhancing the ultimate strength of the hybrid members (Mack et al. 2024).

The composite column can be defined as a compression member manufactured from different types of materials. The outer shell applies a confining pressure that prevents the inner concrete from an early failure, as shown in Figure 1. The shape of the external tube plays a vital role in the confinement effect (Abbas et al., 2021; Abbas and Ali, 2022; Jasim et al., 2024).

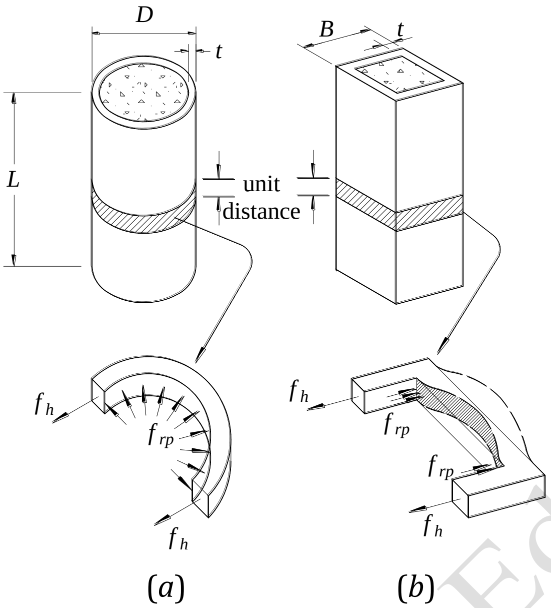

Figure 1 Confinement stress in composite sections (a) circular, and (b) rectangular (Abbas et al., 2024).

The combination of ultra-high-performance concrete UHPC and NC was considered in constructing column specimens by Popa et al. (2014). The column specimens as proposed have a plain UHPC core and reinforced NC shell. The composite columns have an approximately 50% increase in strength than the solid NC columns. The seismic performance of UHPC bridge box piers was investigated using both experimental tests and numerical simulations (Ren et al., 2018). The specimens were simultaneously subjected to constant compressive axial load and cyclic lateral load. It was found that the ductility of box pier specimens will decline with increasing the longitudinal reinforcement ratio. Furthermore, previous studies discussed the merits of hybrid sections with hollow precast concrete tubes filled with core concrete and subjected to cyclic loading (Kim, et al., 2016; Kim et al., 2017, Im et al., 2023). They found that the lateral reinforcement plays a significant role in increasing the ductility of the specimens. The thicker outer shell of the columns had a non-significant effect on the structural behavior of the columns. The ductility, energy dissipation, and stiffness in hybrid sections are close to solid columns.

Wu, et al. (2018) tested five column specimens with UHPC shells and NC cores subjected to concentric axial loads. The loads were applied on the inner core only while the outer shell was stressed indirectly due to the links by threaded bars. They found that lateral reinforcement plays an important role in enhancing the strength, stiffness, energy absorption, and ductility of the hybrid columns. Ridha, et al. (2013) investigated the lightly reinforced RPC columns with concentric loading with and without reinforcement, and they concluded that plain RPC columns are of little higher strength than lightly reinforced RPC columns but with lower ductility. Kadhum and Mankhi (2016) compared the behavior of RPC columns with and without lateral reinforcement. They found that lateral reinforcement plays an important role in increasing the strength of the columns, and the steel fiber content is important in delaying the initiation of the first cracks.

The main objective of this study is to investigate the behavior of hybrid columns manufactured from precast hollow RPC tubes filled with NC and study the change in strength and behavior. Hybrid columns with an outer shell of RPC that works as a shield are more economical than solid RPC columns. The RPC has a high percentage of steel fibers which allows testing how the reinforcement may affect the behavior. It is common in previous researches to apply loads indirectly via using a beam-column connection, enlargement, or fixing a steel collar to the end of the column. The present paper deals with direct edge loads on compression members as may be visualized when the loads are applied directly from girders on the compression members via elastomeric pads resting on a part of the upper face as shown in Figure 2. Also, the present study deals with the load distribution that plays an important role in the contact problems as seen in some applications like load transfer in precast concrete members (Proksch-Weilguni, 2024; Al-Fasih et al., 2024).

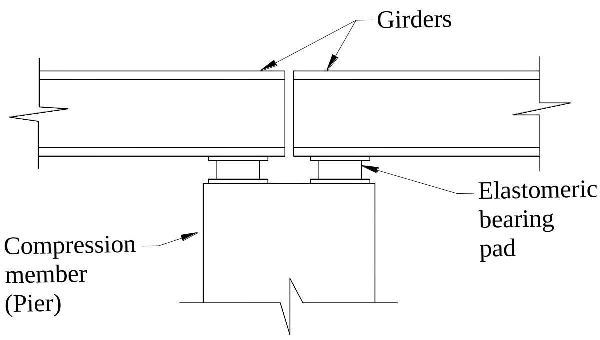

Figure 2 Edge loading on bridge piers.

2. Experimental Program

The experimental work includes casting, preparing, and testing nine specimens of outer dimensions of 180×180×400 mm. These specimens were subjected to eccentric loading. The mechanical properties of the RPC and NC have been obtained first. The ultimate compressive, flexural rupture, and splitting tensile strengths were measured using the standard tests.

2.1 Detail of Specimens

The specimens were divided into three groups, and each group had three specimens. The first group was RPC solid columns, and the other two groups were composed of precast RPC outer walls of 25 and 50 mm filled with normal concrete NC. The aim is to use two categories of RPC tubes with thin and thick walls. Generally, the thickness of the feasible thinner wall is 25 mm, so the steel reinforcement chosen was wires of small size. The second type of RPC is having thick walls that give an economical member. The first specimen in each group was without any reinforcement, while the second specimen was reinforced longitudinally with eight 4 mm deformed bars and laterally with 3 mm undeformed ties spaced 180 mm. The third specimen in each group was reinforced longitudinally with the same number and size of bars while the ties were 90 mm spaced. Figures 3 and 4 illustrate the geometry of the specimens, RPC wall thicknesses, and the details of reinforcements as given in Table 1.

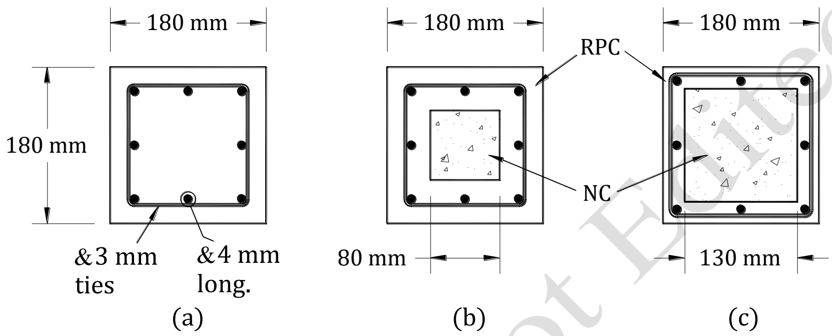

Figure 3 Column specimens, (a) solid column, (b) hollow column with 50 mm thick wall, (c) hollow column with 25 mm thick wall.

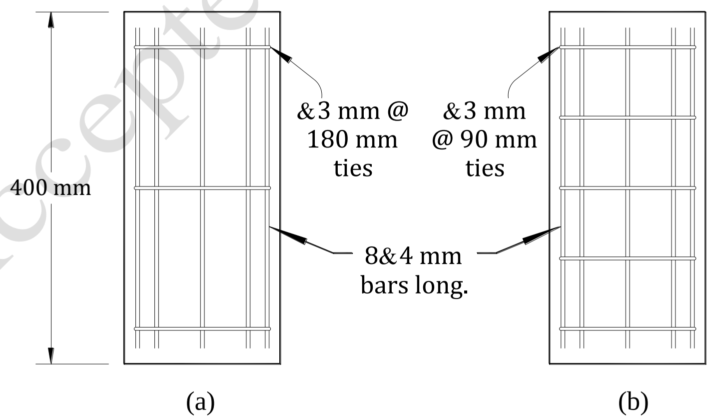

Figure 4 Reinforcement details with 180 mm and 90 mm spacing of ties.

Table 1 Column specimen details

Specimen	RPC shell thickness (mm)	Spacing of ties (mm)
GST3	---	180
GH25T3	25	180
GH50T3	50	180
GST5	---	90
GH25T5	25	90
GH50T5	50	90
GSN	---	---
GH25N	25	---
GH50N	50	---

2.2 Material and Mix Properties

Ordinary Portland cement (ASTM Type I) was used in the production of concrete. The test results showed that the cement complied with the standard provisions. Silica fume has been used as an additive to the RPC mixes with 0.1% maximum chloride content. The partial replacement weight of cement by silica fume was 25% (ASTM C 1240, 2005).

Fine sand known as glass sand with a maximum size of 800 μm was used for the RPC mix, while the NC mix contained fine natural sand of 4.75

mm maximum size and coarse aggregate with 10 mm maximum size. Tables 2 and 3 illustrate the mixes of RPC and NC, respectively. All mixes and the curing process of the specimens used tap water.

Adding a superplasticizer improved the workability and strength of the concrete. The superplasticizer is a third generation that meets the requirements of ASTM C 494 (2005). Mono-filament steel fibers are used with a length of 15 mm and a diameter of 0.2 mm as shown in Figure 5. The description and the properties of the steel fibers are given in Table 4. The specimens are lightly reinforced using 4 mm deformed steel bars for the longitudinal reinforcement, and 3 mm undeformed steel bars for the lateral reinforcement. The tensile test for 4 mm bars gave yielding and tensile strengths of 550 MPa and 603 MPa, respectively, and likewise for 3 mm bars it gave 680 MPa and 749 MPa, respectively.

Table 2 Proportions of constituent materials in RPC mix.

Parameter	**Concrete mix (1 m^3)**
Cement (kg/m^3)	900
Quartz Sand(kg/m^3)	990
Silica fume (kg/m^3)	225
Silica fume % [1]	25%
Water (l/m^3)	157.5

Water to cementitious ratio w/B	0.16
Superplasticizer (kg/m^3)	67.5
Superplasticizer % [2]	6%
Steel fibers (kg/m^3)	156
Steel fibers V_f % [3]	2%

[1] Percentage of weight of cement.

[2] Percentage of cementations materials (cement + silica fume) weight.

[3] Percentage of mix volume.

Table 3 Proportions of constituent materials in NC mix.

Parameter	**Concrete mix (1 m^3)**
Cement (kg/m^3)	460
Fine Aggregate Sand (kg/m^3)	625
Coarse Aggregate Gravel (kg/m^3)	969
Water (l/m^3)	216
W/C Ratio %	0.47

Figure 5 Steel fiber sample

Table 4 Properties of steel fiber

Description	Straight
Length	15 mm
Diameter	0.2 mm
Density	7800 kg/m^3
Tensile strength	2500 MPa
Aspect ratio	75

2.3 RPC and NC Properties

To determine the compressive and splitting tensile strengths for RPC, twelve 100×200 mm cylinders were used. Also, six 100×100×400 mm prisms were prepared and used for determining the flexural strengths of RPC at the age of

28 and 90 days. For NC, six 100×200 mm cylinders and three 100×100×400 mm prisms were tested at 28-day age. Table 5 shows the testing results. Both RPC and NC specimens were cured in a water bath. The results in the table were taken as an average of testing of three specimens with an acceptable deviation as set in the standards. For example, the compressive strengths of 28-day and 90-day age specimens were obtained after a series of trial tests with varying constituent material proportions.

Table 5 Test results of control specimens

Age (days)	**Compressive strength (MPa)**		**Tensile strength (MPa)**		**Flexural strength (MPa)**	
	RPC	**NC**	**RPC**	**NC**	**RPC**	**NC**
28	106.6	38.13	13.1	2.85	18.6	3.9
90	124.0	---	16.6	---	23.8	---

2.4 Specimens Preparing and Testing

The hybrid columns were prepared by vertical casting of RPC mix using plywood molds. Three mold shapes were made from plywood, as shown in Figure 6. After 60 days of curing of RPC tubes as shown in Figure

7, NC was infilled in the voids of the specimens. After another 28 days, all columns became ready for testing and were white painted.

Figure 6 Molds for the column specimens

Figure 7 Column specimen’s outer skin after hardening

Keeping the even, flat, and level surface of the specimen ends is important to ensure uniform loading. The first precaution taken is to keep the evenness of the specimen ends directly after casting the fresh concrete mixes into the molds and allowing the concrete to compact using a convenient compacting process. During the test of specimens, the main parameters of the behavior were recorded at every increasing step of loading. Lateral displacements were measured at the mid-height of the specimen by using two (0.01mm/div.) sensitivity dial gauges of 30 mm capacity attached to the outer faces. Readings from these gauges attached to the column at both loaded and unloaded side faces were recorded for each load stage. Also, a system of demic points was fixed on two opposite sides to get the results of the strains of the section. The columns were tested in a calibrated hydraulic machine of 2500 kN maximum capacity. Figure 8 shows a general view of the eccentric edge load and the distribution of demic points on the section.

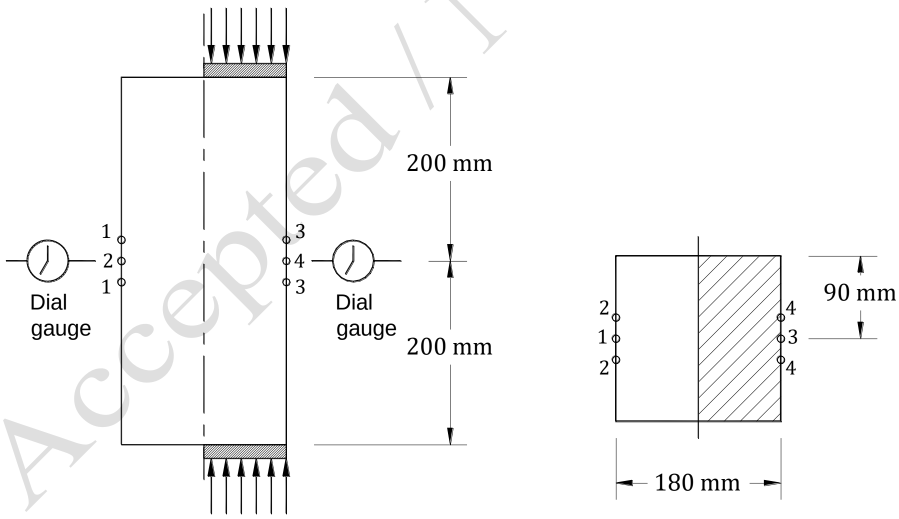

Figure 8 Demec points distribution in edge loaded specimens: (a) side view (b) plan view.

3. Results and Discussions

All specimens were subjected to edge eccentric loads, and the failure loads of all specimens are shown in Table 6. The first observation is that the failure load for the unreinforced hybrid specimens of 50 mm and 25 mm RPC shell thickness (GH50N and GH25N) are less by 46% and 50% of RPC solid column (GSN). It states a clear drop in strength, which is owed to the initial resistance exhibited by compressed walls only while the far side of the wall is almost not contributing to counteracting the compressive stresses. This behavior is in short columns while the long columns are anticipated to behave differently since the distribution of stresses will include the overall section in resisting edge stresses. This encourages extending the present investigation to cover the long columns in future studies.

For the solid specimen (GST3) reinforced with 180 mm spacing ties, the strength reached 1494 kN, while for the hybrid column specimens with similar reinforcement (GH50T3 and GH25T3), the strengths were decreased by 43% and 50%. The strength of the solid specimen (GST5) of 90 mm spacing ties is 1598 kN, while in the hybrid specimens (GH50T5 and GH25T5), the strengths were decreased by 38% and 44% compared to the solid specimen. The above indicates that increasing the wall thickness plays a vital role in raising the ultimate strengths of the specimens, and this behavior will not be affected by providing light reinforcement ratios.

The results of the ultimate loads of the solid specimens indicate that both the longitudinal and lateral reinforcement give a 15%, and 23% increase in the strengths of GST3, and GST5 specimens compared with the unreinforced GSN specimen. Figure 9 shows the vertical strains on both the loaded side 3-3 and unloaded side 1-1, while Figure 10 shows the lateral strains on the loaded side 4-4 and unloaded side 2-2. The load-lateral deflection behavior of solid specimens is shown in Figure 11. The unreinforced specimen was more ductile even with less ultimate failure load. That may be owed to the role of the reinforcement in reducing strains and deflections, which are followed by sudden crushing due to concentrated stress produced from edge loads. This finding involves increasing the steel reinforcement percentages in RPC columns to reduce the probability of sudden failures. The failure pattern of unreinforced specimen GSN is a diagonal crack as shown in Figure 12, which is an indication of no reinforcement that resists inclined stresses induced. The lightly reinforced solid specimens (GST3 and GST5) failed by crushing at the ends without major cracks developed in GST5, which suggests the significance of the lateral reinforcement to reduce the crack widths.

Table 6 Capacity load of tested specimens

Specimen	Capacity Load (KN**)**
GSN	1301

GH25N	648
GH50N	702
GST3	1494
GH25T3	753
GH50T3	846
GST5	1598
GH25T5	897
GH50T5	1002

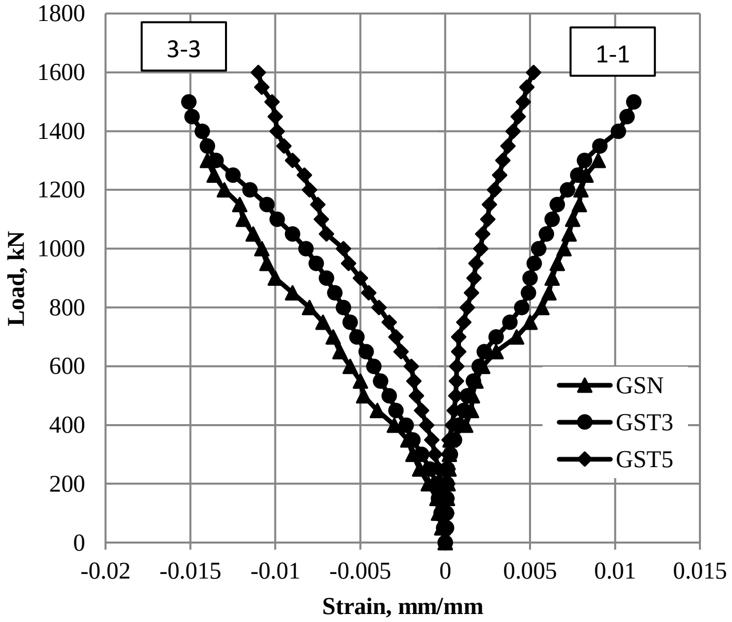

Figure 9 Load-vertical strain relationships for solid specimens

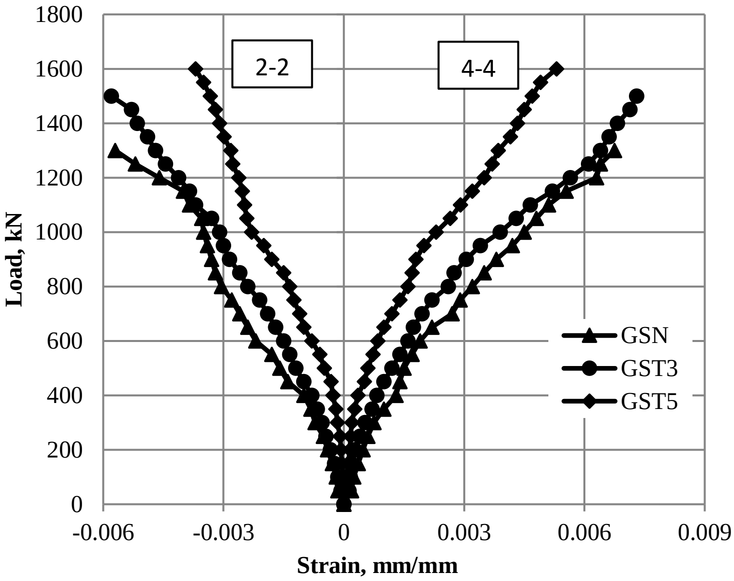

Figure 10 Load-lateral strain relationships for solid specimens

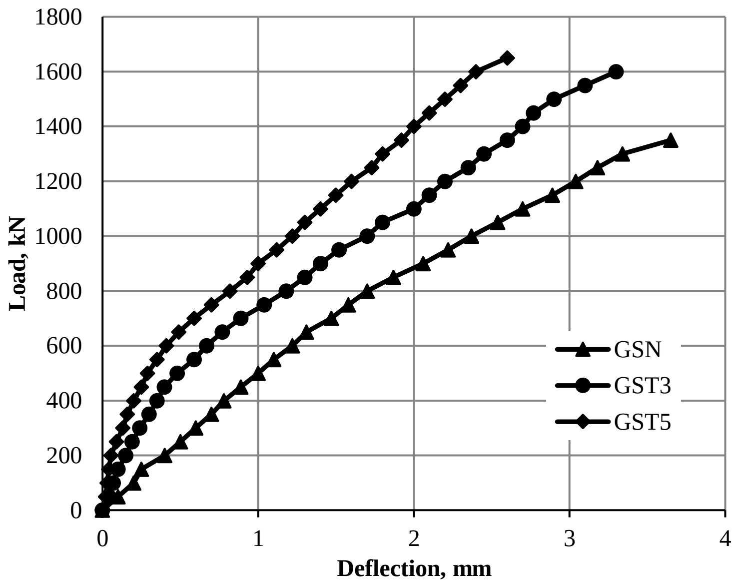

Figure 11 Load-lateral deflection relationships for solid specimens

(a) (b) (c)

Figure 12 Failure modes of solid specimens: (a) Diagonal failure of GSN specimen, (b) End crushing failure of GST3 specimen, and (c) End crushing and bearing failure of GST5 specimen

The hybrid specimen, GH50N, with 50 mm wall thickness and no reinforcement was compared with the lightly reinforced hybrid specimens, GH50T3 and GH50T5. The increase in strengths due to providing reinforcement is 21% and 43%, respectively. The load-vertical strain and load-lateral strain curves are shown in Figures 13 and 14. The load-lateral deflection is shown in Figure 15 where the non-reinforced specimen, GH50N, showed an approximately linear relationship. The strains are initiated linearly and then increased till sudden failure with diagonal cracks in the unreinforced specimen, GH50N, and vertical cracks in the lightly reinforced specimens, GH50T3 and GH50T5, till crushing at the ends, as shown in Figure 16. The crushing at the ends is more apparent in specimen, GH50T3, with less lateral reinforcement of 180 mm spaced ties than in specimen, GH50T5, with 90 mm spacing.

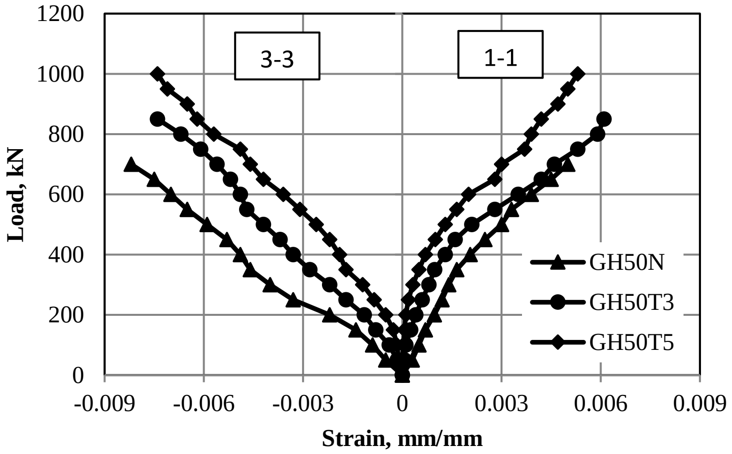

Figure 13 Load- vertical strain relationships for hybrid specimens with 50 mm wall thickness

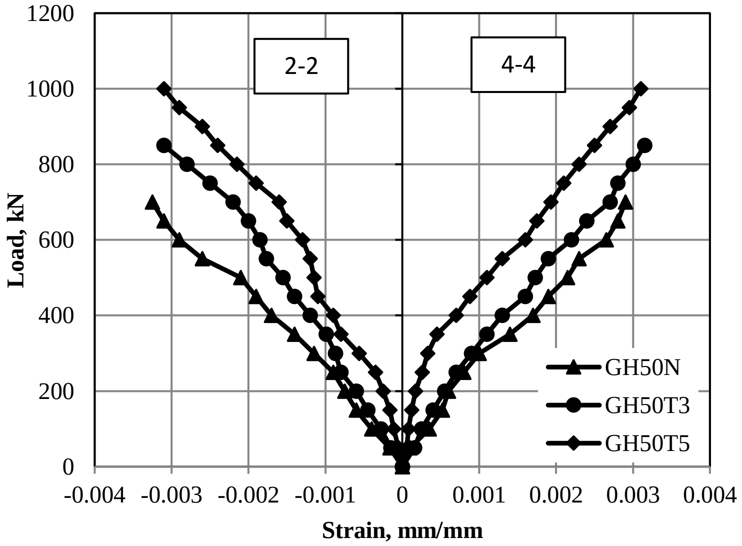

Figure 14 Load- lateral strain relationships for hybrid specimens with 50 mm wall thickness

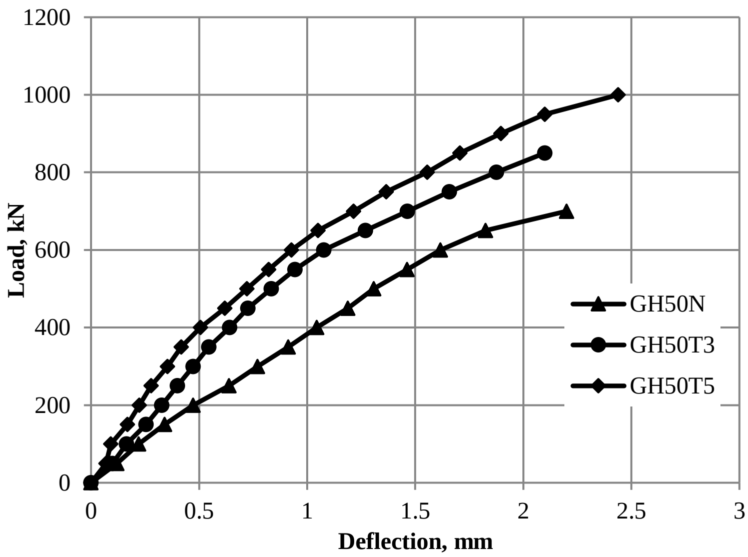

Figure 15 Load-lateral deflection relationships for hybrid specimens with 50 mm wall thickness

(a) (b) (c)

Figure 16 Failure modes of hybrid specimens with 50 mm wall thickness: (a) Diagonal and horizontal cracking failure of GH50N specimen, (b) Vertical cracking failure of GH50T3 specimen, and (c) Vertical cracking failure of GH50T5 specimen

For the specimens with hybrid sections with 25 mm wall thickness (GH25T3 and GH25T5) the reinforcement will increase the strength to 16% and 38% of the unreinforced specimen, GH25N. The load-strain curves are in Figures 17 and 18, where the strains on the loaded side are greater than that on the unloaded. The specimens start with relatively high stiffness till a point where cracks begin to appear. The steel fibers and steel reinforcement resist tensile stresses and try to prohibit the widening of cracks while the stiffness declines moderately. The effect of the light ratio of reinforcement on load-deflection behavior is shown in Figure 19. The failure of the specimens begins with hairline cracks then develops to vertical splitting cracks and ends with crushing at the ends. The patterns of failure are shown in Figure 20.

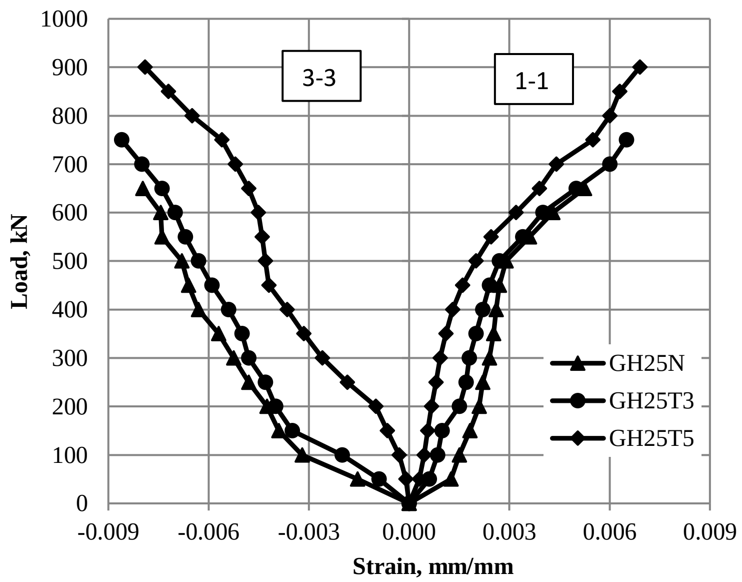

Figure 17 Load- vertical strain relationships for hybrid specimens with 25 mm wall thickness

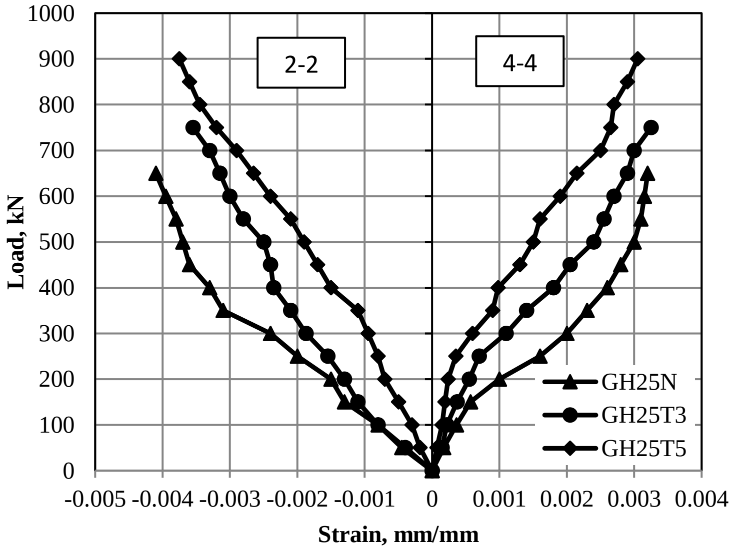

Figure 18 Load- lateral strain relationships for hybrid specimens with 25 mm wall thickness

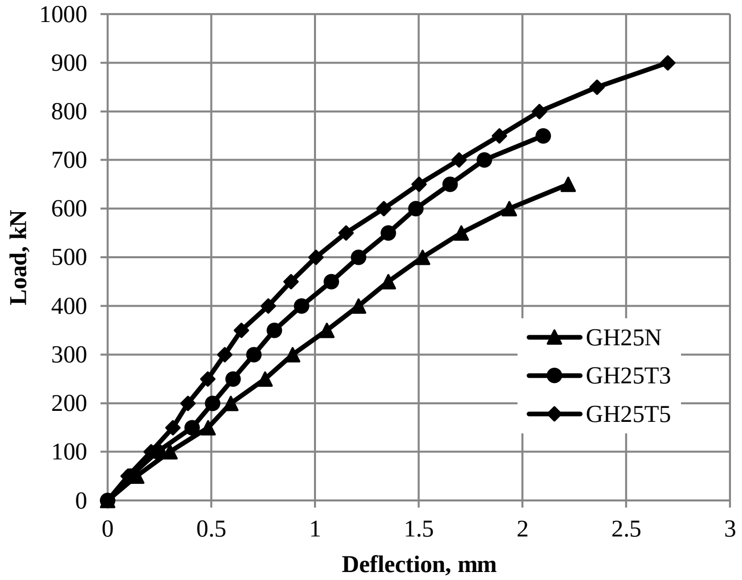

Figure 19 Load-lateral deflection relationships for hybrid specimens with 25 mm wall thickness

(a) (b) (c)

Figure 20 16 Failure modes of hybrid specimens with 25 mm wall thickness: (a) vertical splitting cracking failure of GH25N specimen, (b) Vertical splitting cracking failure of GH25T3 specimen, and (c) Vertical splitting cracking failure of GH25T5 specimen

4. Conclusions

The most important goal of the experimental program in this research is to determine the strength and behavior characteristics of the hybrid compression members subjected to eccentric edge loading. From the experimental tests, the following conclusions are worth mentioning.

As expected, the hybrid specimens gave a lower load capacity than the RPC solid columns. For reinforced solid columns, both the vertical and lateral strains were much higher than those of reinforced hybrid columns. This can be considered as an advantage for the solid members over the hybrid members, which can be beneficial for the load distribution in the case of the partial or patch loading in the compression members. The load distribution is important in some applications like load transfer in precast concrete members. The results showed that the reinforcement will be more effective in the solid specimens and with specimens with larger thicknesses. So, it is recommended to use reinforcement even in minimum percentages to enhance the behavior of RPC columns with eccentric loading.

For all columns, the first cracks of hairline type appeared at the tension face of the mid-height of the specimen and were curbed from further major propagations due to the effect of steel fiber. It was noticed that the first cracks are additionally delayed in the reinforced specimens. The failure was by spalling and crushing at the compression side in the solid and 50 mm thick walled hybrid specimens, while in the 25 mm thick walled specimens, the cracks developed instantaneously at both sides till splitting of the walls and disintegration between the outer RPC shell and the NC core. The contribution of the steel fiber content was clear by reducing the number and spread of the cracks. Due to both the steel fiber and reinforcement effects, the strength and stiffness were increased. In the non-reinforced specimens, a sudden-type failure occurred even with the steel fibers contained. The reinforced solid columns were stiffer than the other types at the initial load stages. The stiffness was increased for the hybrid specimens by increasing the RPC shell thickness from 25 mm to 50 mm. It means that RPC shares in increasing stiffness, and it reduces ductility. In the pre-failure loading stage, the ductility improves for the reinforced solid specimens and the hybrid specimens with the increasing thickness of the RPC shell of the hybrid column specimens. That prompts the recommendation of increasing the steel ratios in conditions of seismic or dynamic loading.

It is recommended to extend the scope of the present study to cover the long columns. The effect of slenderness on the hybrid specimens with edge loading will behave in a different manner. The length of the stress trajectories induced from patch loading will affect the load distribution. It is expected to extend the findings of the present research.

5. References

1. Abbas, N.J. and Ali A.A. (2022). "Prediction of axial capacity of octagonal concrete-filled steel tube columns considering confinement effect", *International Journal of Structural Engineering (IJSTRUCTE)*, 12(2), 170-188, https://doi.org/10.1504/IJSTRUCTE.2022.121891
2. Abbas, N.J., Ali, A.A., Almuhsin, B.S. (2024). "A new approach of estimation of axial strength of composite columns", AIP Conference Proceedings, 3219(1), 020052, https://doi.org/10.1063/5.0237086

3. Abbas, N.J., Abdul-Husain, Z.A. and Ali, A.A. (2021). "Prediction of axial capacity of hexagonal concrete-filled steel tube columns", *2021 International Conference on Advance of Sustainable Engineering and its Application (ICASEA),* Wasit, Iraq, 153-158, https://doi:10.1109/ICASEA53739.2021.9733058.
4. Abdal, S., Mansour, W., Agwa, I., Nasr, M., Abadel, A., Özkılıç, Y. and Akeed, M.H. (2023). "Application of ultra-high-performance concrete in bridge engineering: current status, limitations, challenges, and future prospects", *Buildings*, 13(185), 1-24, https://doi.org/10.3390/ buildings13010185
5. Al-Fasih, M.Y.M., Edris, W.F., Elbialy, S., Marsono, A.K., and Al Sayed, A.A.A., (2024). "Lateral displacement behavior of ibs precast concrete elements reinforced with dual system", *Civil Engineering Journal*, 10(1), 317-335. https://doi.org/10.28991/CEJ-2024-010-01-020
6. ASTM C 1240-05 (2005). "Standard specification for the use of silica fume as a mineral admixture in hydraulic cement concrete, mortar, and grout", *American Society for Testing and Material International*.
7. ASTM C 494-05 (2005). "Standard specification for chemical admixtures for concrete", *American Society for Testing and Material International*.

8. Blais, P.Y. and Couture, M. (1999). “Precast, prestressed pedestrian bridge – world’s first reactive powder concrete structure”, *PCI Journal*, 60-71, https://doi.org/10.15554/PCIJ.09011999.60.71

9. Im, C.R., Kim, S., Yang, K.H., Mun, J.M., Oh, J.H. and Sim, J.I. (2023). “Cyclic loading test for concrete-filled hollow pc column produced using various inner molds”, *Steel and Composite Structures*, 46(6), 793-804, https://doi.org/10.12989/scs.2023.46.6.793

10. Jasim, A.D.A., Wong, L.S., Al-Zand, A.W. and Kong, S.Y. (2024). “Evaluating axial strength of cold-formed c-section steel columns filled with green high-performance concrete”, *Civil Engineering Journal*, 10, *Special Issue, Sustainable Infrastructure and Structural Engineering: Innovations in Construction and Design*, 271-290, https://doi.org/10.28991/CEJ-2023-09-11-020

11. Kadhum, M.M. and Mankhi, B.S. (2016). “Behavior of reactive powder concrete columns with or without steel ties”, *Civil and Environmental Research*, 8(1), 19-26.

12. Kim, C.S., Lee, H.J., Park, C.K., Hwang, H.J. and Park, H.G. (2017). “Cyclic loading test for concrete-filled hollow precast concrete columns produced by using a new fabrication method”, *Journal of Structural Engineering, ASCE*, 143(4), 04016212-1-13, https://doi.org/10.1061/(ASCE)ST.1943-541X.0001703

13. Kim, C.S., Lim, W.Y., Park, H.G. and Oh, J. K. (2016). "Cyclic loading test for cast-in-place concrete-filled hollow precast concrete columns", *ACI Structural Journal*, 113(2), 205–215, https://doi.org/10.14359/51688195
14. Mack, V., Salehfard, R., Habibnejad Korayem, A. (2024). "Comparative study of the effects of key factors on concrete-to-concrete bond strength", *Civil Engineering Infrastructures Journal*, 57(1), pp. 205-223. doi: 10.22059/ceij.2023.353447.1903
15. Moslehi, A., Dashti Rahmatabadi, M.A. and Arman, H. (2023). "Determination of optimized mix design of reactive powder concrete", *Advances in Civil Engineering*, 4421095, https://doi.org/10.1155/2023/4421095
16. Popa, M., Constantinescu, H., Zagon, R., Kiss, Z. and Bolca, G. (2014). "Experimental tests performed on concrete columns with ultra-high performance fibre reinforced cores", *Journal of Applied Engineering Sciences*, 17(1), 67-73.
17. Proksch-Weilguni, C., Decker, M., and Kollegger, J. (2024). "Load distribution and passive confinement in reinforced concrete: Development of a mechanical model", *Engineering Structures*, 304, 117562, https://doi.org/10.1016/j.engstruct.2024.117562.

18. Ren, L., Fang, Z., Zhong, R., Wang, K. (2018). “Experimental and numerical investigations of the seismic performance of UHPC box piers”, *KSCE Journal of Civil Engineering*, 23(2), 597-607, https://doi.org/10.1007/s12205-018-0567-8

19. Ridha, M.M.S., Ali, T.K.M. and Abbawi Z.W. (2013). “Behavior of axially loaded reactive powder concrete columns”, *Journal of Engineering and Development*, 17(2), 193-209.

20. Salahuddin, H., Qureshi, L.A., Nawaz, A. and Raza, S.S. (2020). “Effect of recycled fine aggregates on performance of reactive powder concrete”, *Construction Building Materials Journal*, 243, 118223, https://doi.org/10.1016/j.conbuildmat.2020.118223.

21. Wang, C., Xue, G. and Zhao, X. (2021). “Influence of fiber shape and volume content on the performance of reactive powder concrete (RPC)”, *Buildings*, 11(7), 286, https://doi.org/10.3390/buildings11070286.

22. Wu, X., Kang, T.H.-K., Mpalla, I.B., and Kim C.-S. (2018). “Axial load testing of hybrid concrete columns consisting of UHPFRC tube and normal-strength concrete core”, *International Journal of Concrete Structures and Materials*, 12, 43, https://doi.org/10.1186/s40069-018-0275-2